Use of an improved radiation amplification factor to estimate the effect of total ozone changes on action spectrum weighted irradiances and an instrument response function

Jay R. Herman[1,2]

Received 12 May 2010; revised 27 July 2010; accepted 1 September 2010; published 9 December 2010.

[1] Multiple scattering radiative transfer results are used to calculate action spectrum weighted irradiances and fractional irradiance changes in terms of a power law in ozone Ω, $U(\Omega/200)^{-RAF}$, where the new radiation amplification factor (RAF) is just a function of solar zenith angle. Including Rayleigh scattering caused small differences in the estimated 30 year changes in action spectrum-weighted irradiances compared to estimates that neglect multiple scattering. The radiative transfer results are applied to several action spectra and to an instrument response function corresponding to the Solar Light 501 meter. The effect of changing ozone on two plant damage action spectra are shown for plants with high sensitivity to UVB (280–315 nm) and those with lower sensitivity, showing that the probability for plant damage for the latter has increased since 1979, especially at middle to high latitudes in the Southern Hemisphere. Similarly, there has been an increase in rates of erythemal skin damage and pre-vitamin D_3 production corresponding to measured ozone decreases. An example conversion function is derived to obtain erythemal irradiances and the UV index from measurements with the Solar Light 501 instrument response function. An analytic expressions is given to convert changes in erythemal irradiances to changes in CIE vitamin-D action spectrum weighted irradiances.

Citation: Herman, J. R. (2010), Use of an improved radiation amplification factor to estimate the effect of total ozone changes on action spectrum weighted irradiances and an instrument response function, *J. Geophys. Res.*, *115*, D23119, doi:10.1029/2010JD014317.

1. Introduction

[2] All biological processes and most materials exposed to sunlight on the Earth's surface are affected by changes in the amount of solar ultraviolet radiation (280–400 nm) caused by changing ozone amounts, cloud-aerosol transmission, and scattering back to space. Laboratory measurements have been made to quantify these effects, both for absolute effect in terms of the incident irradiance and for the relative effect of each wavelength in a specified range λ_1–λ_2. The relative effect is usually specified in terms of a normalized weighting function, or action spectrum $A(\lambda)$, for the incident irradiance $F_1(\lambda, \theta, \Omega, t, C_T)$ as a function of wavelength λ, solar zenith angle θ, ozone Ω, time t, and cloud transmission C_T. Although not giving an absolute rate of biological change or materials damage, the action spectrum approach to determine a production-effect $P(\theta, \Omega, t, C_T)$ (equation (1)), can be used to estimate relative change from a reference state of irradiance $F_2(\lambda, \theta, \Omega_2\ t, C_T)$ caused by changes in ozone amount and cloud plus aerosol transmission [*Herman*, 2010; *Madronich et al.*, 1998; *McKinlay and Diffey*, 1987; *Setlow*, 1974; *Setlow et al.*, 1993]. Long-term trends can be estimated for time-dependent processes related to $A(\lambda)$ under the assumption that the effect is linear with the amount of irradiance, or that the nonlinearity is known. An example of the latter is for some biological processes where a saturation level is reached and further exposure to UVB irradiance does not proportionately produce the same effect [*Hollis et al.*, 2007; *Bogh et al.*, 2010; *Camacho et al.*, 2010]. This study will only consider the linear regime.

$$P(\Omega,\theta,t,C_T) = \int_{\lambda_1}^{\lambda_2} F(\lambda,\theta,\Omega,t,C_T)A(\lambda)d\lambda \qquad (1)$$

The units of $P(\theta, \Omega, t, C_T)$ are taken to be the same as $F(\lambda, \theta, \Omega, t, C_T)\ d\lambda$, since $A(\lambda)$ is dimensionless and normalized to 1 at some wavelength λo, usually near 300 nm. In this study the units of P are watts/m^2. However, the normalizations of $A(\lambda)$ are not standard, which can cause the magnitude of $P(\theta, \Omega, t, C_T)$ to vary with the assumed normalization. Exceptions are the standardized normalization of CIE erythemal $A_{ERY}(\lambda)$, CIE pre-vitamin D3 A_{VIT}, and the UV index derived from $P_{ERY}(\theta, \Omega, t, C_T)$ as 40 P_{ERY} when F$d\lambda$ is in W/m^2. Although the nonstandard normalizations of

[1]University of Maryland, Baltimore County, Joint Center for Earth Systems Technology, Baltimore County, Maryland, USA.
[2]Now at Goddard Space Flight Center, Greenbelt, Maryland, USA.

0148-0227/10/2010JD014317

$A(\lambda)$ do not affect the estimations of percent change of the various $P(\theta, \Omega, t, C_T)$ over time t, the wavelength range over which each $A(\lambda)$ is defined does affect the percent change.

[3] Understanding, modeling, and measuring the factors that affect the amount of UV and visible radiation reaching the Earth's surface are important because changes in radiation amounts impact agricultural and ocean productivity, global energy balance, and human health. Increases in UV dose affect human health adversely through skin cancer [*Diffey*, 1991], eye cataracts [*Taylor*, 1990], and suppression of the immune system [*Vermeer et al.*, 1991], yet positively, for the same typical exposure time, through the increased rate of vitamin D production [*Grant*, 2002; *Holick*, 2004]. Changes in UV radiation also significantly affect ecosystem biology [*Smith et al.*, 1992; *Ghetti et al.*, 2006] and the rate of damage to various materials exposed to sunlight.

[4] For wavelengths shorter than 280 nm (UVC), almost no solar photons reach the Earth's surface because of ozone (Hartley and Huggins bands) and molecular oxygen absorption (Schumann-Runge bands and continuum absorption). Photons with wavelengths in the UVB (280–315 nm) and UVA (315–400 nm) ranges do reach the Earth's surface as a fraction of the incident solar irradiance at the top of the atmosphere $I_0(\lambda, t)$. Aside from clouds and aerosols, there is significant attenuation of I_0 by ozone in the wavelength range $\lambda < 330$ nm. For example, there is strong absorption at 310 nm, where a 1% change in ozone leads to an approximate 1% change in irradiance for $\theta = 45°$. At wavelengths less than 310 nm, the increasingly large ozone absorption coefficient leads to a proportionally larger percent increase in irradiance for a small percent decrease in ozone (e.g., at $\theta = 45°$, a 1% decrease in ozone can produce a 2.2% increase in 305 nm irradiance). This scaling function is frequently described as a "radiation amplification factor $RAF(\theta,\Omega)$ that can take different functional forms depending on the specific process and whether the process considered depends on a range of wavelengths or is approximately monochromatic.

[5] The inverse relation between ozone changes and UVB irradiance changes is well established by both theory and measurements [*Latarjet*, 1935; *Bener*, 1972; *Madronich*, 1993a; *Bodhaine et al.*, 1997; *Micheletti et al.*, 2003] based on the laboratory measured ozone absorption coefficients and radiative transfer calculations through a Rayleigh scattering atmosphere with ozone absorption. In the approximation where scattering is represented by an extinction optical depth $\tau_E(\lambda,p) = \tau_R + \tau_A$, for Rayleigh and aerosol extinction, the amount of solar radiation F reaching the Earth's surface for a solar zenith angle θ and column ozone amount Ω (milli-atm-cm) can be estimated from Beer's law, $F = I_o \exp(-\alpha\Omega\sec(\theta) - \tau_E \sec(\theta))$, where α is the ozone absorption coefficient (cm^{-1}). Changes in F caused by changes in Ω can be estimated from equation (2) with RAF $(\theta,\Omega_2) = -\alpha\Omega_2 \sec(\theta)$, where Ω_2 is a reference value of ozone amount, and Ω_1 is a time varying amount. For the $\sec(\theta)$ approximation, θ should be less than 70°.

$$(F_1 - F_2)/F_2 = \exp(-\alpha\Omega_2 \sec(\theta)(\Omega_1 - \Omega_2)/\Omega_2) - 1. \quad (2)$$

For processes that are affected by exposure to solar ultraviolet irradiance, the daily amount of UV radiation (290–330 nm) changes with the seasons and latitude (solar zenith angle or airmass effect), the amount of aerosols in the atmosphere, the amount of cloud plus aerosol transmission C_T, the amount of ozone, and the Sun-Earth distance. The changes in $P(t,\theta, \Omega)$ have been discussed for long-term zonal average changes in Ω and C_T [*Herman*, 2010] for four common action spectra but neglecting scattering. These four action spectra are erythemally weighted irradiances A_{ERY} [*McKinlay and Diffey*, 1987], CIE pre-vitamin D_3 production A_{VIT} [*Bouillon et al.*, 2006], plant growth response A_{PLA} [*Flint and Caldwell*, 2003], and the DNA damage function A_{DNA} [*Setlow*, 1974]. An equation for estimating action spectrum weighted changes in $P(t,\theta,\Omega)$ for changes in Ω is given by equation (3), which can be numerically obtained from equation (2) for each action spectrum (Figure 1) or from multiple scattering radiative transfer solutions, for $200 < \Omega < 600$ DU. Equation (3) provides a new definition of the RAF that is not dependent on the amount of ozone (Figure 2 and Appendix Figures A1–A3).

$$P(\theta, \Omega) = U(\theta)(\Omega/200)^{-RAF(\theta)} \text{ or } P_{12}/P_2 = (\Omega_{12}/\Omega_2 + 1)^{-RAF(\theta)} - 1. \quad (3)$$

The calculated weighted irradiances $P(\theta, \Omega)$ are obtained from relatively fast scalar radiative transfer calculations of irradiance (e.g., the TUV model [*Madronich*, 1993b; *Madronich and Flocke*, 1997] or the SBDART model [*Ricchiazzi et al.*, 2004]), with both including the effects of Rayleigh scattering and spherical geometry corrections for $\theta > 60°$. For erythemal irradiance $RAF_{ERY}(\theta < 10°) = 1.25$ from Beer's Law without scattering and 1.20 with scattering from the TUV model, with mid-latitude O_3-profile shape, and 0.05 surface reflectivity.where $P_1 = P(t, \theta, \Omega_1)$, $P_2 = P(t, \theta, \Omega_2)$, $P_{12} = P_1 - P_2$, and $\Omega_{12} = \Omega_1 - \Omega_2$. For the action spectra in Table 1, the scaling coefficient $U(\theta)$ ($watts/m^2$) and radiation amplification factor $RAF(\theta)$ are determined as fitting parameters to the TUV radiative transfer calculations of the variation in $P(t, \theta, \Omega_1)$ and the solar zenith angle SZA = θ. Nine $A(\lambda)$ functions are shown in Figure 1. The tabulated solutions are expressed as functional fits that are uniform with an $r^2 > 0.9999$ for $U(\theta)$ and $RAF(\theta)$. All calculations in this paper are done with TUV radiative transfer model estimated irradiances as a function of Ω and θ for cloud-free and aerosol-free conditions.

[6] This study extends the analysis of *Herman* [2010] for additional action spectra $A(\lambda)$ and effect-production functions $P(\theta, \Omega)$ that are sensitive to changes in ozone amount (Table 1) over the ozone range $200 < \Omega < 600$ DU. All of the calculations and functional fits are given in terms of irradiances instead of irradiance ratios. $RAF(\theta)$ values and associated 30 year irradiance changes are estimated including Rayleigh scattering. UV trend estimates assume local noon conditions, where Ω and θ vary with latitude and day of the year for the period 1979–2008. One of the action spectra, $A_{DNA}(\lambda)$ has been modified from that previously used to match the data used in the TUV radiative transfer program. The changes are in the UVA (320–400 nm) portion of the spectrum, which are not significantly affected by ozone changes.

[7] The UVB-dominated plant action spectrum A_{PLC} [*Caldwell*, 1971] is discussed separately and compared with the more recent UVB and UVA plant action spectrum A_{PLA}

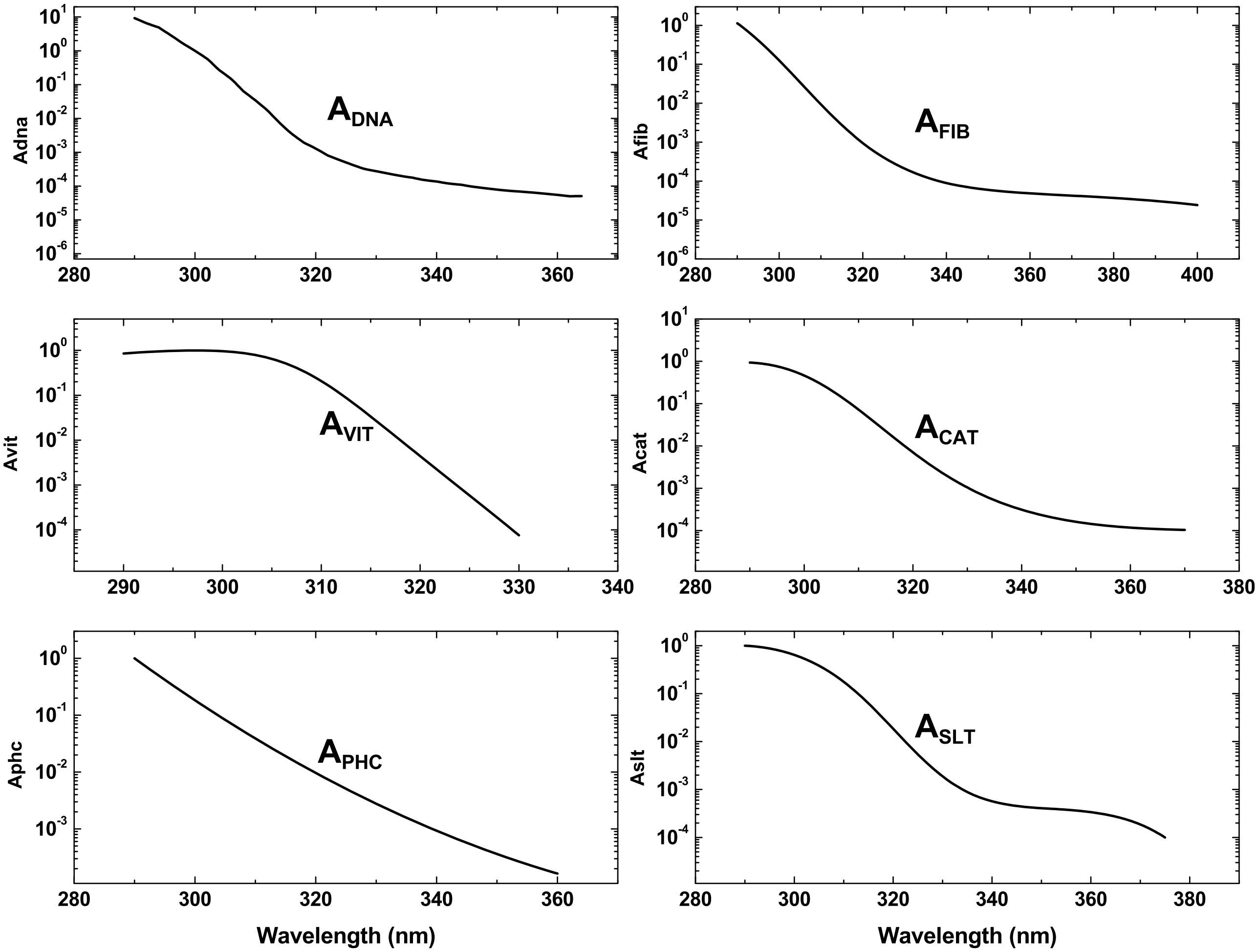

Figure 1. Six action spectra corresponding to Table 1. The functional fits to these spectra are given in the Appendix Table A1.

given by *Flint and Caldwell* [2003]. Finally, the RAF power law form is obtained for a manufacturer supplied instrument response function $R_{SLT}(\lambda)$. This permits the conversion of irradiances and irradiance changes measured by a typical Solar Light 501 broadband instrument to irradiances weighted by the standard CIE erythemal action spectrum or to the UV index. Additionally, an expression is given for the conversion of measured erythemal irradiance to irradiance weighted by the CIE vitamin D action spectrum.

2. Parameterization of RAF(θ) and U(θ)

[8] Equation (1) is used to integrate each fitted action spectra A(λ) (Appendix Table A1) times the calculated irradiances F(λ,Ω,θ) over the specified wavelength range (Table 2) for each ozone value and solar zenith angle in the ranges $200 < \Omega < 600$ DU and $0° < \theta < 80°$. The TUV radiative transfer results are summarized in the functional form given by equation (3) in terms of U(θ) and RAF(θ). The fitting coefficients are given in Table 2 and the corresponding graphs for nine of the U(θ) and RAF(θ) shown in Figure 2. The small error bars in Figure 2 represent the nonlinear least squares fitting error to the tabulated values of RAF(θ) and U(θ). Of more interest is an estimate of the residuals from using equation 3 compared to the calculated weighted irradiance values.

[9] An example of the TUV erythemal irradiance calculation is shown in the Appendix (Figure A1) for the range $200 < \Omega < 600$ DU and $0° < \theta < 80°$. Figure A2 shows the residuals obtained using equation (3) compared to the TUV erythemal irradiance calculation. For all of the spectra considered in this study, the residuals are less than 1%. The maximum to minimum residuals R overall θ, Ω values are given in Table 2 column 1. The residuals at any specific Ω are $R/4$ as a function of θ. Although the RAF calculated from equation (3) is independent of the ozone amount, Figure A3 shows that the common definition RAF*(θ,Ω) = $\log(I_1/I_2)/\log(\Omega_2/\Omega_1)$ is dependent on the ozone amount. The new RAF is harder to calculate but easier to use for estimation of irradiances or change in irradiances.

[10] All of the U(θ) and RAF(θ) fitting functions have been checked to have continuity of values and slope to where TUV spherical geometry corrected solutions are valid (θ = 83°). The scaling coefficients U(θ) represent the irradiance values at Ω = 200 DU. The RAF(Ω) coefficients for four of the action spectra (ERY, VIT, PLA, DNA) are slightly different than those given previously [*Herman*,

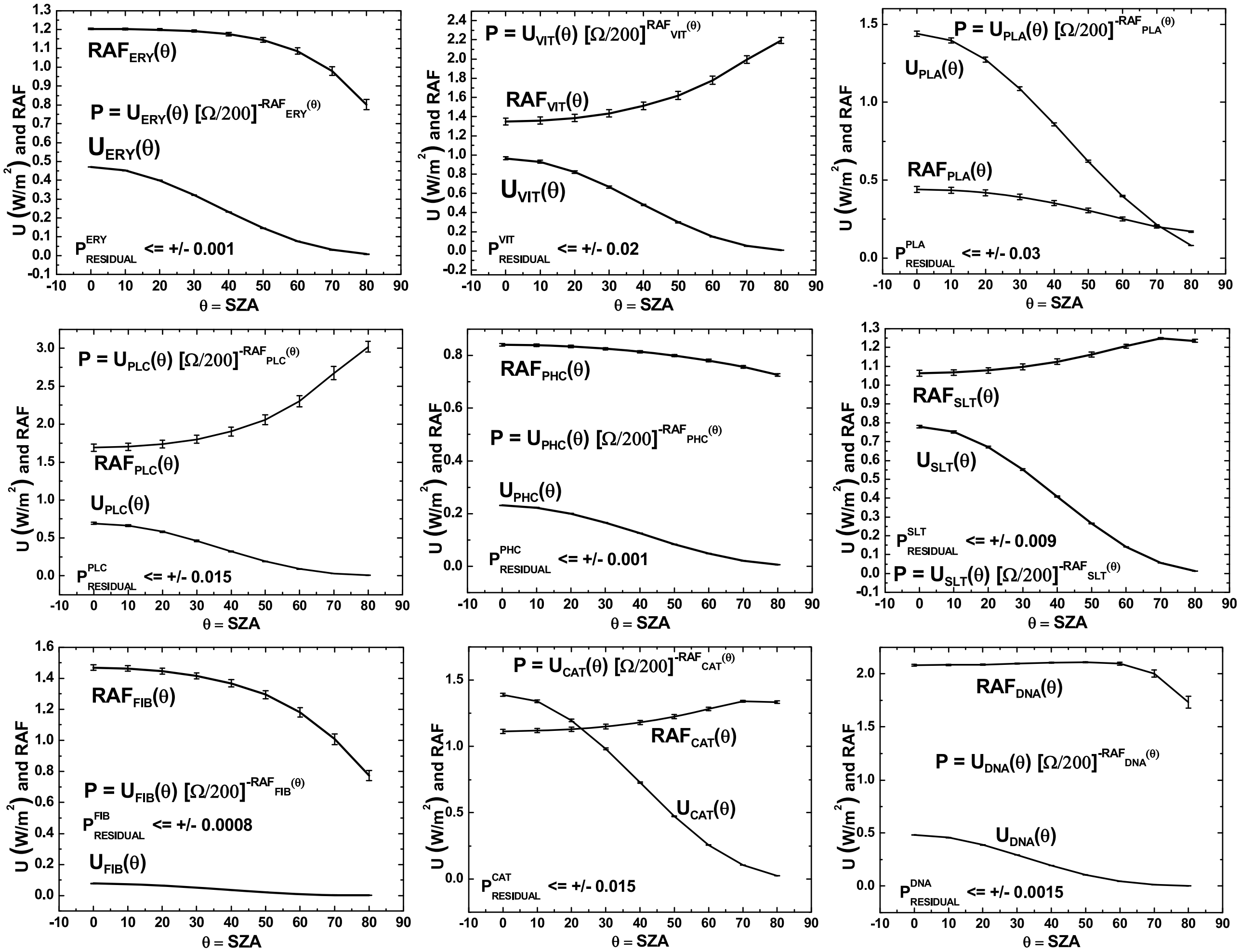

Figure 2. RAF(θ) and U(θ) fitting functions corresponding to weighted irradiances P for 9 action spectra (Table 1) and equation (3) using the TUV radiative transfer calculation with U(θ) having dimensions of Watts/m^2.

2010] based on Beer's law calculations without Rayleigh scattering.

[11] The functional fit to erythemal $P_{ERY}(\theta,\Omega)$ has been compared to measurements in terms of the RAF(θ) associated with the power law function. Comparisons show that the power law form (equation (3)) approximately matches measured broadband erythemal irradiance data [*Booth and Madronich*, 1994; *Blumthaler et al.*, 1995; *Bodhaine et al.*, 1997; *Herman*, 2010].

3. Plant Action Spectra A_{PLA} and A_{PLC}

[12] Two different plant action spectra have been described that are similar in the UVB portion of the spec-

Table 1. Action Spectra for Various Processes

Symbol	Process	Reference
A_{FIB}	1. Inactivation of human fibroblasts	*Tyrrell and Pidoux* [1987]
A_{PHC}	2. Inhibition of phytoplankton carbon fixation	*Boucher et al.* [1994]
A_{PHP}	3. Inhibition of photosynthesis in Antarctic phytoplankton	*Cullen and Neale* [1997]; *Neale and Kieber* [2000]
A_{MOC}	4. Skin cancer in albino hairless mice corrected for human skin	*Gruijl et al.* [1993]
A_{NAC}	5. Damage to eggs and larvae of northern anchovy	*Hunter et al.* [1979]; *Smith and Baker* [1982]
A_{CAT}	6. In vitro UV-induced cataract using whole lenses	*Oriowo et al.* [2001, 2002]
A_{PLC}	7. Plant growth function in the UVB range	*Caldwell* [1971]
A_{PLA}	8. Plant growth function (UVB and UVA)	*Flint and Caldwell* [2003]
A_{VIT}	9. CIE pre-vitamin D_3 production	*Bouillon et al.* [2006]
A_{ERY}	10. CIE erythemal	*McKinlay and Diffey* [1987]
A_{DNA}	11. UV DNA damage (TUV fit)	Setlow
R_{SLT}	12. Solar Light 501 response function	Solar Light Corporation

Table 2. Radiation Amplification Factors RAF(θ) and Scaling Coefficient U(θ)[a]

Action Spectra	U(θ) (W/m^2)	RAF(θ)
DNA damage	a = 0.4808619129703342	a = 2.081686042925178
U_{DNA} & RAF_{DNA}	b = 0.0002581388722413753	b = −0.0002564844392747189
$R < \pm0.0015$	c = −0.00013015618956397	c = −0.0005162843529327841
	d = 3.363099051664871E-08	d = 1.96876012322816E-08
	e = 9.038404614651682E-09	e = 3.556832243378462E-08
	f = 9.879488073283888E-12	f = −1.129759402996411E-13
Fibroblasts	a = 0.07800680713750653	a = 1.467889155998693
U_{FIB} & RAF_{FIB}	b = 0.0002071976414471761	b = −0.0002064058786479314
$R < \pm0.0008$	c = −1.979645705714768E-05	c = −0.0003550824599259368
	d = 2.846880662657818E-08	d = 1.169161007843218E-08
	e = 1.290375602439486E-09	e = 2.232625244026806E-08
	f = 2.553133582980263E-12	f = −6.052119118575507E-14
CIE pre-vitamin D	a = 0.9659616883022778	a = 1.349378286522954
U_{VIT} & RAF_{VIT}	b = 0.0001089314449687077	b = −0.0002926808443875372
$R < \pm0.02$	c = −0.0002681987275053843	c = −0.0003059282407232034
	d = 1.410783665933483E-08	d = 2.879164470755759E-08
	e = 1.894213900598701E-08	e = 1.920553492457117E-08
	f = 1.695104643516458E-12	f = −8.580442654658103E-13
CIE erythemal	a = 0.4703918683355716	a = 1.203020609002682
U_{ERY} & RAF_{ERY}	b = 0.0001485533527344676	b = −0.0001035585455444773
$R < \pm0.001$	c = −0.0001188976502179551	c = −0.00013250509260352
	d = 1.915618238117361E-08	d = 4.953161533805639E-09
	e = 7.693069873238405E-09	e = 1.897253186594168E-09
	f = 1.633190561844982E-12	f = 0.0
Cataracts	a = 1.389543317864509	a = 1.11438721946406
U_{CAT} & RAF_{CAT}	b = 0.0001111136998782643	b = −0.0002058168034144146
$R < \pm0.015$	c = −0.0003539100981229902	c = −0.0001923468030173855
	d = 1.068457231439126E-08	d = 1.356704548496917E-08
	e = 2.29621042619638E-08	e = 1.028553859915792E-08
	f = 1.575202883621628E-12	f = −3.874776677975742E-14
Inhibition of phytoplankton carbon fixation	a = 0.2312193698282898	a = 0.8401845037386215
U_{PHC} & RAF_{PHC}	b = 0.0001028838438585395	b = 0.0002655900976547904
R < ±0.001	c = −5.733376829791965E-05	c = 0.0002054127624271793
	d = 8.64812321062776E-09	d = −1.152481680543294E-08
	e = 3.623419099041137E-09	e = −1.309398235637854E-08
	f = 1.210627299169194E-13	f = 1.330268056308169E-14
Flint and Caldwell plant damage	a = 1.438980254099905	a = 0.4420411644303329
U_{PLA} & RAF_{PLA}	b = 0.0001005808369726184	b = −9.318666734881831E-05
$R < \pm0.03$	c = −0.0002894199664477857	c = −9.585567686290419E-05
	d = 5.643194851731751E-09	d = 6.07232152503975E-09
	e = 1.410638475278906E-08	e = 7.54644705023143E-09
	f = 4.226223146491366E-13	f = 5.967599892201557E-13
Caldwell plant damage	a = 0.6929604575774898	a = 1.690988020287883
U_{PLC} & RAF_{PLC}	b = 0.0001501495712857719	b = −0.0002228727044010645
$R < \pm0.015$	c = −0.0001942686727612605	c = −0.0002664325743080134
	d = 1.552691797694485E-08	d = 1.180456040656832E-08
	e = 1.385331244399262E-08	e = 6.748005699490438E-09
	f = 4.373135769713131E-12	f = 1.129962809191574E-13
Solar Light 501 meter	a = 0.7789413669516511	a = 1.062677180507659
U_{SLT} & RAF_{SLT}	b = 9.999108483918942E-05	b = −0.0002244228821673299
$R < \pm0.009$	c = −0.0002040763375327788	c = −0.0002019877480424064
	d = 1.132773753129348E-08	d = 1.6418056756421E-08
	e = 1.363109731632696E-08	e = 1.062982390141093E-08
	f = 8.74102272069114E-13	f = −2.665322212237153E-13

[a]For $0 < \theta < 80°$ and $200 < \Omega < 600$ DU for $P(\Omega,\theta) = U(\theta)\,(\Omega/200)^{-RAF(\theta)}$ U(θ) or $RAF(\theta) = (a + cx^2 + ex^4)/(1 + bx^2 + dx^4 + fx^6)$ $r^2 > 0.9999$. x = θ and 1.0E10 = 1.0×10^{10}.

trum (Figure 3): one with no UVA response [A_{PLC} *Caldwell*, 1971] and the other with UVA response [A_{PLA} *Flint and Caldwell*, 2003].

[13] The processes represented by A_{PLA} and A_{PLC} have very different responses to change in ozone amount. This can be seen by comparing the derived RAF(θ) for the two cases (Figure 4). The distinction is important for plants with extreme sensitivity to the UVB portion of the spectrum, such as certain strains of wheat or tobacco plants [*Bader and Refat*, 1999], where, in general, increased exposure to UVB decreases yields of the crop plant. Some cultivars of soybeans have also been found to be more responsive to the UVB portion of the spectrum with almost no response to UVA.

[14] According to *Mazza et al.* [2000], "the activity spectrum for the induction of UV absorbing sunscreens in soybean appears to have a sharp increase in quantum efficiency below 325 nm, resembling the generalized plant

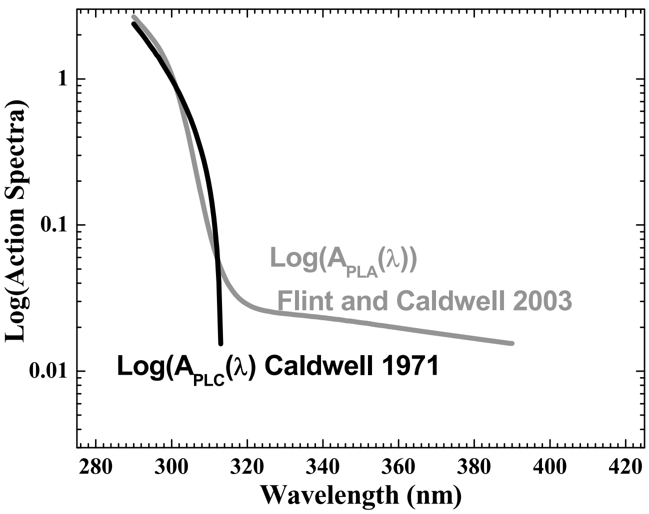

Figure 3. A_{PLC} [*Caldwell*, 1971] and A_{PLA} [*Flint and Caldwell*, 2003].

action spectrum [*Caldwell*, 1971], which assumes very little activity in the UV-A region." *Rousseaux et al.* [1999] showed that a common native species in the southern portions of South America suffered increased DNA damage during the periodic episodes of ozone reduction associated with the overpass of the Antarctic ozone hole. The observed damage was well correlated with the *Caldwell* [1971] type action spectrum A_{PLC} instead of A_{PLA}. Although this effect was recognized [*Searles et al.*, 2001], it was concluded that "only a few subtle plant responses to enhanced UV-B simulating stratospheric ozone depletion were seen in this meta-analysis of 62 field-based research papers published over 20 years." However, on the basis of the studies of *Mazza et al.* [2000] and *Rousseaux et al.* [1999], which showed plant changes for larger changes in ozone, it is of interest to compare the 30 year increases in UV irradiance weighted by A_{PLA} and A_{PLC}.

[15] Because of its sharp cutoff at 313 nm and narrow wavelength range, the RAF(θ) derived from $A_{PLC}(\Omega,\theta)$ increases strongly with θ in a manner similar to the monochromatic 305 nm RAF(θ,Ω), which is proportional to the airmass factor sec(θ) for $\theta < 60°$ (equation (2)). For $\theta > 60°$, the increase in the spherical geometry airmass factor is slower than sec(θ). This contrasts with the $RAF_{PLA}(\theta)$ derived from $A_{PLA}(\lambda)$, which shows low sensitivity to UVB irradiance changes (Figure 5) over a wider SZA range. Plants that have response functions similar to that given by A_{PLA} [*Flint and Caldwell*, 2003] should show little effect for ozone changes compared to those with response functions similar to A_{PLC}.

[16] The 30 year change with ozone (1979–2008) is calculated from the change in zonal average ozone as a function of month and latitude in the same manner as that of *Herman* [2010]. The results (Figure 5) show that plants that are very sensitive to UVB should have experienced considerable more damage in recent years compared to 30 years ago, especially for those that grow at higher latitudes. The effect is much more pronounced in the Southern Hemisphere where the ozone decreases have been larger.

4. Broadband Instrument Estimation of Erythemal Irradiances and Irradiance Change

[17] Biological processes, or broadband instrument measurements, that are sensitive to UVB radiation have a similar functional sensitivity to ozone changes that can be derived through radiative transfer studies [*McKenzie et al.*, 2004]. They showed that the erythemal irradiance (or UV index) measured at the Earth's surface could be related to $UVB_{280–315\ nm}$ and to measurements by various instruments to within 10% using low-order polynomial fitting functions, if the sensitivity to ozone amount (i.e., Ω^{-RAF}) is close to that for erythemal irradiance. For other processes (e.g., Vitamin D production, $UVB_{280–320\ nm}$, DNA damage), they derived correction tables as a function of ozone and solar zenith angle.

[18] The U(θ), RAF(θ) approach is useful for determining long-term trends in erythemal irradiance from broadband instruments or relating the change in vitamin D production or DNA damage from the widely archived UV index. The method is described by relating the irradiance or change in irradiance measured with an instrument's response function to the erythemal irradiance or change in terms of the RAF(θ) and U(θ) functions. The method can be applied to any process where the irradiance or change in irradiance can be described by equations (2) or (3) (e.g., the CIE pre-vitamin D_3 action spectrum A_{VIT}). An alternate approach to deriving correction factors for broadband instrument irradiance measurements relative to the erythemal irradiance is given by *Seckmeyer et al.* [2005] as part of a general discussion of these instruments. Their results are given as graphical functions of solar elevation angle and Ω.

[19] There are a number of broadband instruments designed to measure irradiances that have a response function that approximates the erythemal action spectrum as a

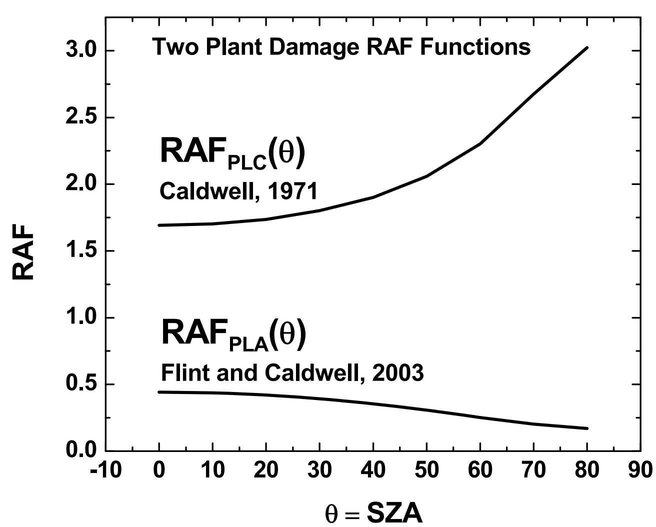

Figure 4. A comparison of the sensitivity to ozone change in terms of the RAF(θ) factors corresponding to A_{PLA} and A_{PLC} of Figure 3.

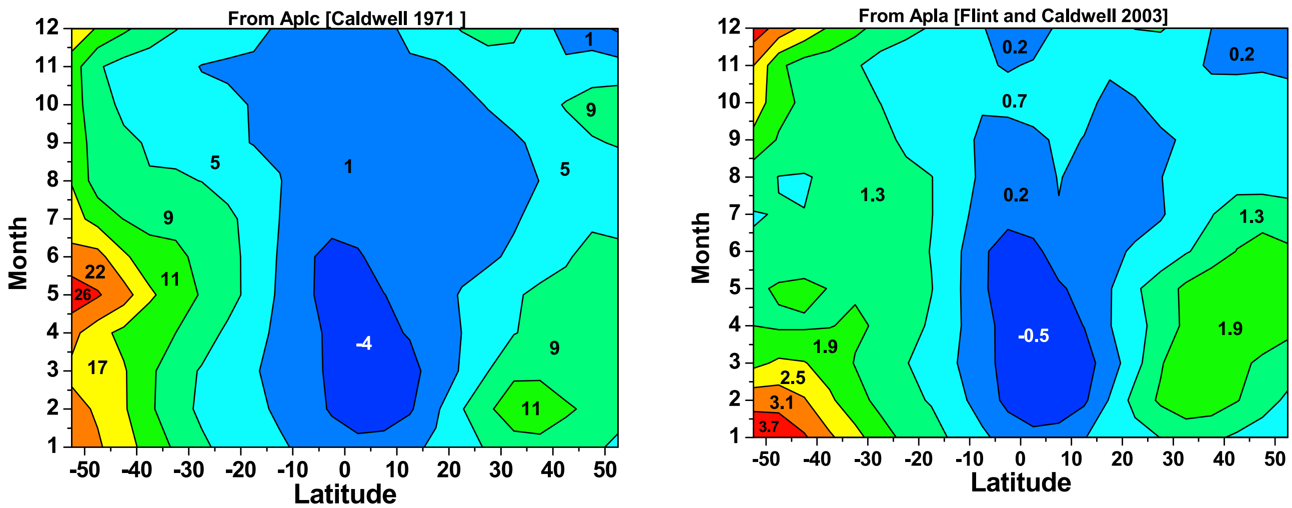

Figure 5. Thirty year change in plant effect P_{PLC} (left) and P_{PLA} (right) as a function of latitude and month for the ozone time series used in the study by *Herman* [2010] from 1979 to 2008 calculated using TUV radiative transfer.

function of wavelength. One of these is the Solar Light 501 meter, which has a manufacturer-supplied response function R_{SLT} shown in Figure 6, with its fitting equation and coefficients given in Table 2, and corresponding RAF_{SLT} and U_{SLT} given in Table 3. Because $R_{SLT}(\lambda)$ is only an approximation to the erythemal action spectrum (Figure 6), the instrument might have a different response to irradiance changes caused by changes in atmospheric ozone amounts than it would if its response function were exactly the erythemal action spectrum $A_{ERY}(\lambda)$.

[20] Equation 3 applies equally well to wavelength dependent action functions or instrumental response functions. If $P_E = P_{ERY}(\theta,\Omega)$ is the effect function (equation (1)) for erythemal irradiance and $P_S = P_{SLT}(\theta,\Omega)$, the effect function for an action spectra identical to the Solar Light 501 response function R_{SLT}, then

$$P_E/P_S = U_E/U_S\left[\Omega/20\tilde{0}\right]^{(RAF_S - RAF_E)} \tag{4a}$$

$$P_{1E}/P_{2E}/(P_{1S}/P_{2S}) = (\Omega_1/\Omega_2)^{RAFS_E} \tag{4b}$$

$$(\Delta P/P_2 + 1)_{ERY} = (\Delta P/P_2 + 1)_{SLT}(\Delta\Omega/\Omega_2)^{RAF_S} \tag{4c}$$

where

$$P_{1E} = P_{ERY}(\theta,\Omega_1) \text{ and } P_{2E} = P_{ERY}(\theta,\Omega_2)$$

$$P_{1S} = P_{SLT}(\theta,\Omega_1) \text{ and } P_{2S} = P_{SLT}(\theta,\Omega_2)$$

$$RAF_{SE} = RAF_{SLT} - RAF_{ERY}$$

$$U_{ES} = U_E/U_S$$

$$\Delta P/P_2 = (P_1 - P_2)/P_2$$

$$\Delta\Omega/\Omega_2 = (\Omega_1 - \Omega_2)/\Omega_2.$$

Equation (4a) gives the direct conversion of Solar Light 501 measured irradiances to erythemal irradiances, if the values of θ,Ω are known. If the SLT irradiance time series $P_{1SLT}(t)$ is known and a reference value is selected P_{2SLT} from this time series, then the equivalent time series for ERY can be formed from equation (4b) or (4c), $P_{1ERY}(t)/P_{2ERY}$. The change in erythemal irradiance caused by ozone changes can now be estimated from the SLT time series. The value P_{2SLT} and P_{2ERY} can be any meaningful, but related, quantity. In a multiyear time series, it might be selected as the value computed from average ozone using the first year's data.

[21] The dimensionless functions $U_{ES}(\theta)$ and $RAF_{SE}(\theta)$ are shown in Figure 7a with fitting functions given in Table 3, or they can be obtained directly from Table 2. Similar conversion functions can be derived for any instrument response function or action spectrum that significantly overlap (e.g., $U_{VE}(\theta)$ and $RAF_{EV}(\theta)$ for erythemal and pre-vitamin D3).

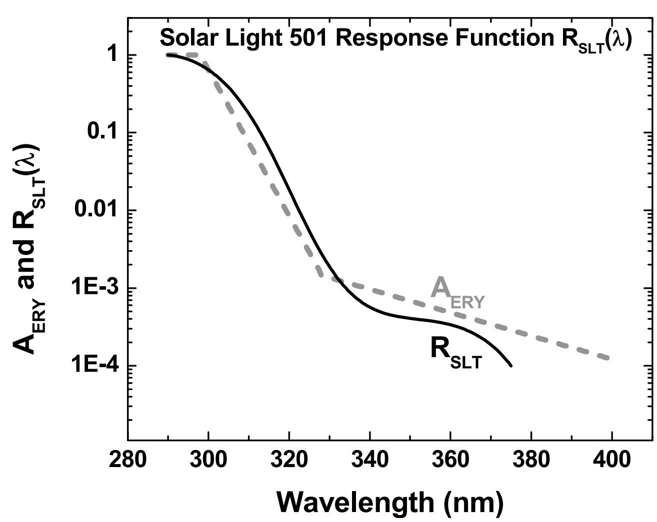

Figure 6. The response function $R_{SLT}(\lambda)$ give by Solar Light Inc. for the 501 m compared to the erythemal action spectrum $A_{ERY}(\lambda)$.

Table 3. Effective Radiation Amplification Factors $RAF_{xy}(\theta)$ and Scaling Coefficient[a]

Action Spectra	U(θ)	RAF(θ)
Solar Light to erythemal	$U_{ES} = (a + cx + ex^2)/(1 + bx + dx^2 + fx^3)$	$RAF_{SE} = (a + cx^2 + ex^4)/(1 + bx^2 + dx^4)$
U_{ES} & RAF_{SE}	a = 0.603917044048268	a = −0.1403825493062795
Solar Light to erythemal	b = −0.01672027539360061	b = −0.0001719518706435208
	c = −0.01012833503237699	c = 6.888444890305315E-05
	d = 0.0001084602755626854	d = 1.162406670651049E-08
	e = 4.530445856312848E-05	e = −3.359090891961678E-09
	f = −4.150188333357393E-07	
Erythemal to vitamin-D	$U_{VE} = (a + cx^2 + ex^4)/(1 + bx^2 + dx^4)$	$RAFev = (a + cx^2 + ex^4)/(1 + bx^2 + dx^4)$
U_{VE} & RAF_{EV}	a = 1.240188751483111	a = −0.146311229501849
	b = −0.0001809408437773429	b = −0.0001980709971345768
	c = −0.0002555096930008766	c = −6.836827401663642E-05
	d = 1.067372208198107E-08	d = 1.202792672184166E-08
	e = 1.439750611757012E-08	e = 6.609409195614681E-09

[a]For $U_{xy}(\theta)$ for $0 < \theta < 80°$ and $200 < \Omega < 600$ DU for $P_{xy} = U_{xy}(\theta)\ (\Omega/200)^{RAFyx(\theta)}$ (equations (4a) and (5a)) ($x = \theta$ 1.0 E 10 = 1.0×10^{10}).

[22] The RAF(θ) values for the Solar Light 501, erythemal action spectrum, and CIE pre-vitamin D3 RAF(θ) functions are compared in Figure 8 showing the different sensitivities to ozone change as a function of SZA. Although the SLT response spectrum is an approximation to the ERY action spectrum, the sensitivities to ozone change are significantly different, especially at large θ. That is, the erythemal radiation amplification factor indicates a value of 1.2 compared to 1.06 for $RAF_{SLT}(\theta)$ for $\theta < 20°$, which means that for an increase in ozone the SLT instrument would measure a smaller decrease in irradiance than the actual change in erythemal irradiance or the UV index (proportional to the erythemal irradiance). If there had been significant ozone changes at low to midlatitudes (between 0° and 35°), the SLT instrument would underestimate those changes by about 14%, especially in the late spring and summer months. The reverse would occur at high latitudes, with the SLT instrument overestimating changes. At latitudes between 40° and 60°, the overestimate would occur mostly in the winter months. The error can be corrected using equation (4). When the measured zonal average 30 year ozone change is used to estimate the change in P_{ERY} and P_{SLT} from A_{ERY} and R_{SLT}, the results are almost identical because of the specific latitude distribution of the observed ozone change.

[23] A similar calculation based on equation (3) can be applied to any broadband instrument response function or process action function encompassing UVB and UVA such as those given in a review of nine broadband instruments [*Vuilleumier and Gröbner*, 2005], which show similar response functions to those instruments produced by Solar Light. A larger analysis of instrument response functions is given in a report by *Vilaplana et al.* [2009] and in an article by *Hülsen and Gröbner* [2007]. In practice, the instrument response function must be measured for each individual instrument, which will likely differ from the manufacturer supplied average response function for a particular instrument model.

[24] An analysis [*Fioletov et al.*, 2009] relating measured erythemal to CIE pre-vitamin D_3 irradiances has been developed based on measured Brewer spectrometer data. This analysis gives an empirical relationship between the ratio R of erythemal action spectrum weighted irradiance and vitamin D action spectrum-weighted irradiance as a

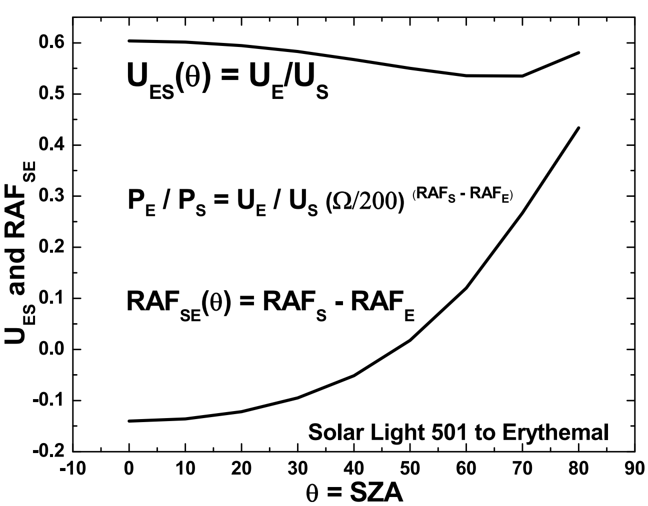

Figure 7a. The effective scaling coefficient U_{ES} and radiation amplification factor RAF_{SE} for converting measured irradiance values from the Solar light 501 meter into those that would result from the CIE erythemal action spectrum.

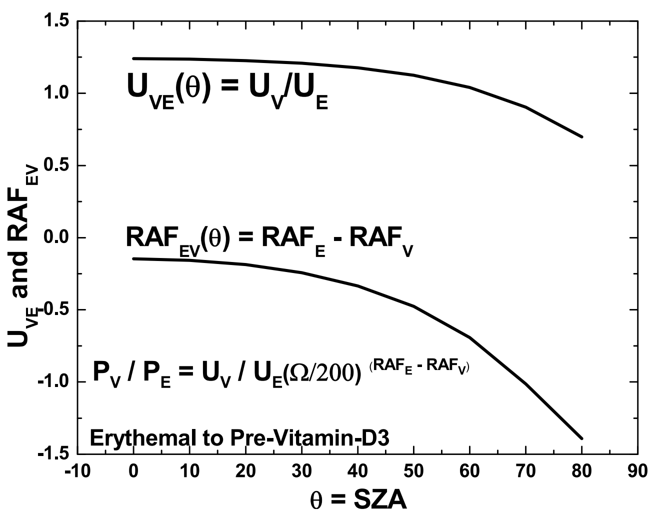

Figure 7b. The effective scaling coefficient U_{VE} and radiation amplification factor RAF_{EV} for converting measured values of erythemal irradiance change into those that would result from the CIE vitamin D_3 action spectrum weighting.

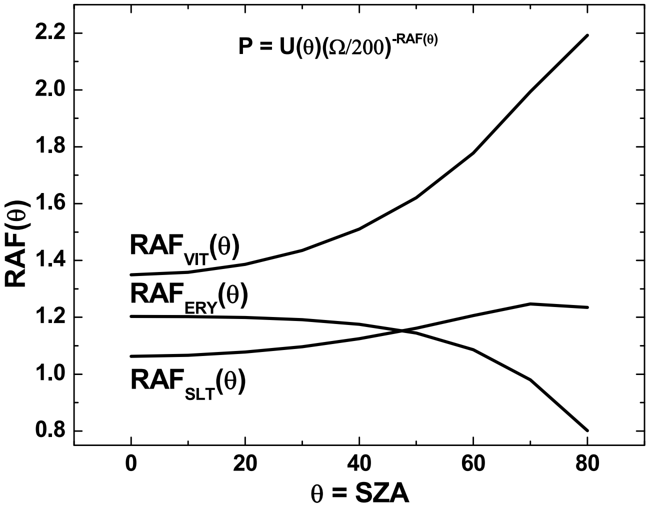

Figure 8. A comparison of $RAF_{SLT}(\theta)$ and to the corresponding functions for erythemal and CIE vitamin D_3-weighted irradiances.

function of ozone amount and solar zenith angle [*Fioletov et al.*, 2009, Figures 5b and 6].

[25] Similarly, the RAF method, using equation (4b) or (4c), can be applied to converting measurements of the erythemal spectrum into a process represented by a different action spectrum. Equation (5a) permits the vitamin D3-weighted irradiance to be determined from measurements of erythemal irradiance. In the example below, estimates of erythemal irradiance change caused by changes in ozone are related to changes represented by the CIE pre-vitamin D_3 action spectrum-weighted irradiances. The calculated change in A_{VIT}-weighted irradiances from measured changes in erythemal irradiance can be estimated in terms of RAF_{EV} fitting function given in Table 3 and Figure 7b. The change $(\Delta P/P_2 + 1)_{VIT}$ can be estimated using equation (5b).

$$P_V/P_E = U_V/U_E[\Omega/200]^{(RAF_E - RAF_V)} \quad (5a)$$

$$(\Delta P/P_2 + 1)_{VIT} = (\Delta P/P_2 + 1)_{ERY}(\Delta\Omega/\Omega_2 + 1)^{RAF_{EV}}, \quad (5b)$$

where, similar to equation (4),

$$RAF_{EV} = RAF_{ERY} - RAF_{VIT} \text{ and}$$

$$U_{VE} = U_{VIT}/U_{ERY}.$$

The effect of the larger RAF_{VIT} (Figure 8) can be seen when comparing the 30 year change caused by ozone changes (Figure 9). The changes in P_{VIT} and P_{ERY} are similar in form because both corresponding action spectra A_{VIT} and A_{ERY} have strong UVB sensitivity to ozone change. However, the magnitude is quite different, especially at higher latitudes where RAF_{ERY} is much less than RAF_{VIT}.

5. Summary

[26] Calculated irradiances have been obtained corresponding to nine action spectra as a function of ozone amount and solar zenith angle using the TUV radiative transfer program. The calculated action spectrum-weighted irradiances are approximated with a power law given by equation (3). The new radiation amplification factors RAF (θ), and corresponding scaling coefficients U(θ), have been derived for each action spectrum weighed irradiance. Including scattering, a standard midlatitude ozone profile shape, and a surface reflectivity of 0.05 caused small changes in the RAF(θ) functions (e.g., from 1.25 to 1.20 for erythemal irradiance $0 < \theta < 20°$). Changes in the RAF functions also caused small differences in the estimated 30 year change in erythemal and pre-vitamin D_3-weighted irradiances.

[27] Long-term (1979–2008) irradiance changes were compared for two versions of the plant growth inhibition action spectra (A_{PLC} [*Caldwell*, 1971], A_{PLA} [*Flint and Caldwell*, 2003]), the first having sensitivity only in the UVB range (280–315 nm) and the second having sensitivity in both UVA (315–400 nm) and UVB ranges. The results are given in terms of the RAF(θ) functions, which show

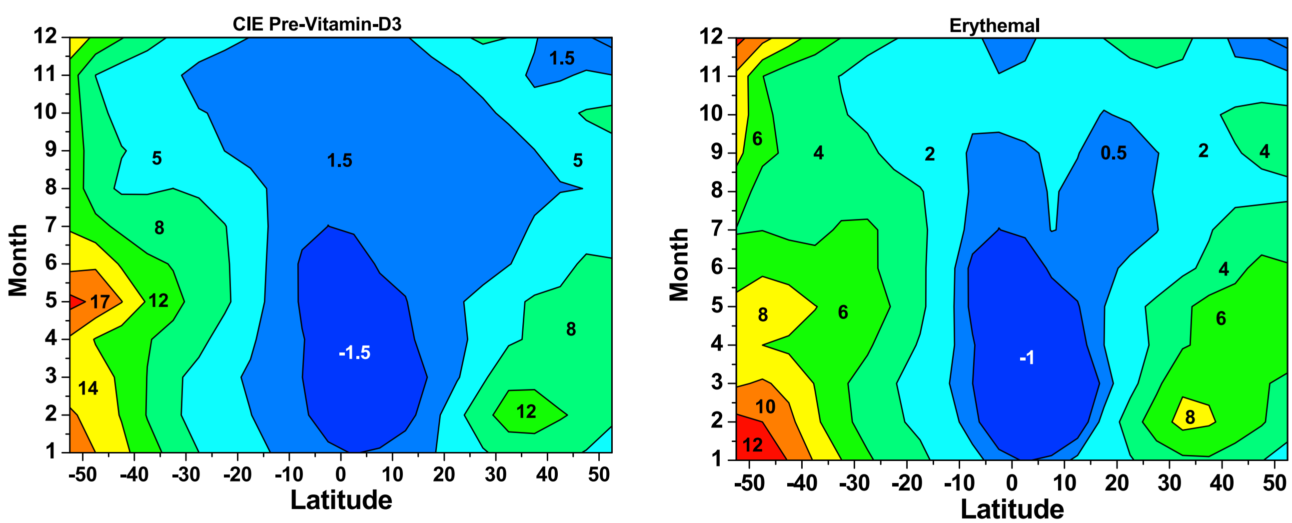

Figure 9. The 30 year change in irradiance weighted (left) by the CIE pre-vitamin D3 action spectrum and (right) by the erythemal action spectrum based on TUV radiative transfer calculations.

larger values for $RAF_{PLC}(\theta)$ than for $RAF_{PLA}(\theta)$. This causes the estimated ozone-related changes in weighted irradiances to be much larger for P_{PLC} than for P_{PLA}, which implies that certain species of plants (e.g., some UVB-sensitive wheat crops, some cultivars of soybean, and especially tobacco) will suffer a larger ozone-related increase in damage or growth inhibition than plants with a strong UVA response in addition to the UVB response.

[28] The $RAF(\theta)$ and $U(\theta)$ formulation was used to assess the effect of estimating long-term erythemal irradiance trends using a broadband instrument response function that only approximates the erythemal action spectrum. The Solar Light 501 is shown to estimate a smaller irradiance change for a given ozone change than the actual erythemal irradiance change. For the 30 year ozone change observed by satellites [*Stolarski and Frith*, 2006], the broadband instrument response function R_{SLT} underestimates by 5% at high Southern Hemisphere latitudes and by 2%–3% at midlatitudes. Correction functions $U_{ES}(\theta)$ and $RAF_{SE}(\theta)$ have been derived for R_{SLT} and could easily be derived for any other response functions with sensitivity in both UVB and UVP plus UVA ranges. As an example, the same method was applied for the conversion of measured erythemal irradiance change into the change in CIE vitamin D-weighted action spectrum irradiance caused by changes in ozone amount using the 30 year ozone time series.

Appendix A

[29] Table A1 gives the fitting functions for action and response spectra listed in Table 1 and used in equation (1). The TUV radiative transfer model was used to calculate the erythemal irradiance reaching the Earth's surface as a function of Ω and θ (see Figures A1). The resulting irradiances $P(\Omega,\theta)$ were fit using a power law, $P(\Omega,\theta) = U(\theta)(\Omega/200)^{-RAF(\theta)}$, where $U(\theta)$ has the dimensions of W/m^2. The fitting residual is ± 0.001 W/m^2 in the worst case, $P(\theta = 50°, \Omega = 200) = 0.15$ W/m^2. The residuals are shown for erythemal irradiance (Figure A2). Other SZA cases have similar but smaller residuals.

[30] As shown in Figure A3, $RAF^*(\theta,\Omega) = \log(I_1/I_2)/\mathrm{Log}(\Omega_2/\Omega_1)$ shows a dependence on ozone and solar zenith

Table A1. Fitting Functions for Action and Response Spectra Listed in Table 1

Action Spectrum	Notation: 5E-05 = 5×10^{-5} x = λ (nm)	
$\mathrm{Log}(A_{DNA})$	$= (a + cx^2 + ex^4 + gx^6 + ix^8)/(1 + bx^2 + dx^4 + fx^6 + hx^8)$	
DNA Damage	a = −0.02641223385787823	f = −3.416197445630558E-15
256 < x < 364 nm	b = −3.724469760845681E-05	g = 4.675691096965972E-15
	c = 1.650914148765947E-05	h = 8.429525867187894E-21
	d = 5.299362685316457E-10	i = −1.550047210015691E-20
	e = −4.754222192303955E-10	
$\mathrm{Log}(A_{FIB})$	$= (a + cx + ex^2)/(1 + bx + dx^2 + fx^3)$	
Fibroblasts	a = −0.6743605747504754	d = 2.174578156447749E-05
290 < x < 400 nm	b = −0.008179149107201934	e = −1.002667143482033E-05
	c = 0.005200102068945352	f = −1.831722649385483E-08
$\mathrm{Log}(A_{VIT})$	$= (a + cx^2 + ex^4 + gx^6 + ix^8)/(1 + bx^2 + dx^4 + fx^6 + hx^8 + jx^{10})$	
CIE pre-vitamin D_3	a = −2.206561655915826	f = −9.823081504492026E-15
250 < x < 330 nm	b = −4.920810458194582E-05	g = 1.258709968255984E-14
	c = 9.913601195747653E-05	h = 4.929270593670856E-20
	d = 9.798814014662167E-10	i = −3.557334134380907E-20
	e = −1.673792457228989E-09	j = −9.835295140251223E-26
A_{ERY}	1 x < 298 nm	
CIE Erythemal	$10^{(0.094E0*(298.-x))}$ 298 < x < 328 nm	
298 < x < 400 nm	$10^{(0.015E0*(139.-x))}$ 328 < x < 400 nm	
	0 > x > 400 nm	
$\mathrm{Log}(A_{CAT})$	$= (a + cx^{0.5} + ex)/(1 + bx^{0.5} + dx)$	
Cataracts	a = −2.907765524151222	d = 0.003239849768263829
250 < x < 330 nm	b = −0.1136450635225155	e = −0.01006931775553438
	c = 0.3422166680190406	
$\mathrm{Log}(A_{PHC})$	$= (a + cx^{0.5} + ex)/(1 + bx^{0.5} + dx)$	
Phytoplankton Carbon Fixation	a = −21.62765029748863	d = 0.004496947123947301
290 < x < 368 nm	b = −0.1384882915848433	e = −0.06594594302039233
	c = 2.393012441617194	
$\mathrm{Log}(A_{PLA})$	$= (a + cx^{0.5} + ex + gx^{1.5})/(1 + bx^{0.5} + dx + fx^{1.5})$	
Plant Growth	a = −2.747345187913439E0	e = −0.0276281414383589E0
285 < x < 390 nm	b = −0.1791837870949891E0	f = −0.000211935199455902E0
	c = 0.4771127256925517E0	g = 0.000533462299874 1222E0
	d = 0.01068245009604864E0	
$\mathrm{Log}(A_{PLC})$	$= (a+cx+ex^2+gx^3)/(1+bx+dx^2+fx^3)$	
Plant Growth	a = 3.575797064847171	e = 0.0001079715734682457
290 < x < 313 nm	b = −0.008235859905070269	f = −1.915810086119585E-08
	c = −0.03404813752625744	g = −1.140295361160647E-07
	d = 2.210204319173256E-05	
$\mathrm{Log}(A_{SLT})$	$= (a + cx^{0.5} + ex + gx^{1.5})/(1 + bx^{0.5} + dx + fx^{1.5} + hx^2)$	
Solar Light 501	a = 0.0417103636337212	e = 0.000338737539908666
275 < x < 375 nm	b = −0.2219180239342533	f = −0.0006801066573862663
	c = −0.006561111341913155	g = −5.712754413689448E-06
	d = 0.01844120116219344	h = 9.392020090729325E-06

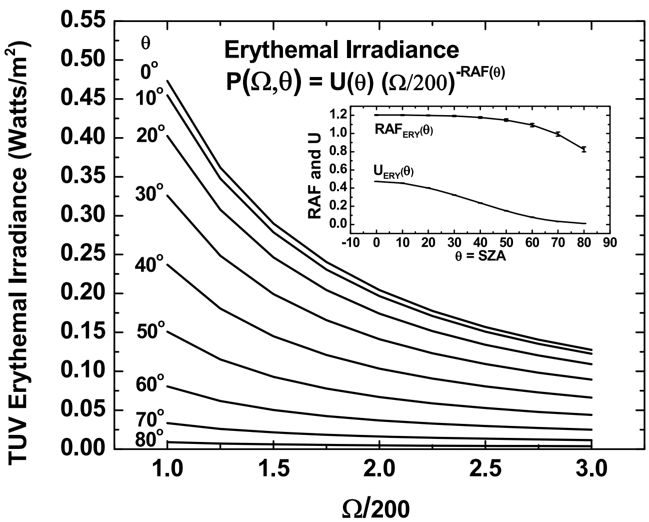

Figure A1. Erythemal irradiance $P_{ERY}(\Omega,\theta)$ (W/m^2) calculated from the TUV radiative transfer model for a range of ozone and SZA, $200 < \Omega < 600$ DU and $0° < \theta < 80°$. The inset graph contains the RAF(θ) and U(θ) needed for the fit P(Ω,θ). At noontime summer solstice at 40° latitude with 350 DU of ozone P(U,RAF, Ω) is approximately 0.22 ± 0.001 W/m^2. For clear skies, this corresponds to a UV index of 8.8 ± 0.04. $U_{ERY}(\theta)$ has the units of W/m^2.

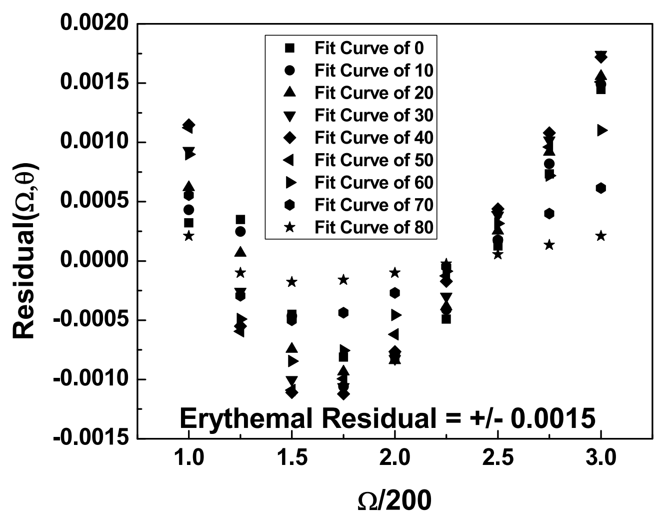

Figure A2. Residuals between the TUV erythemal irradiance calculation and the power law approximation as a function of θ and Ω.

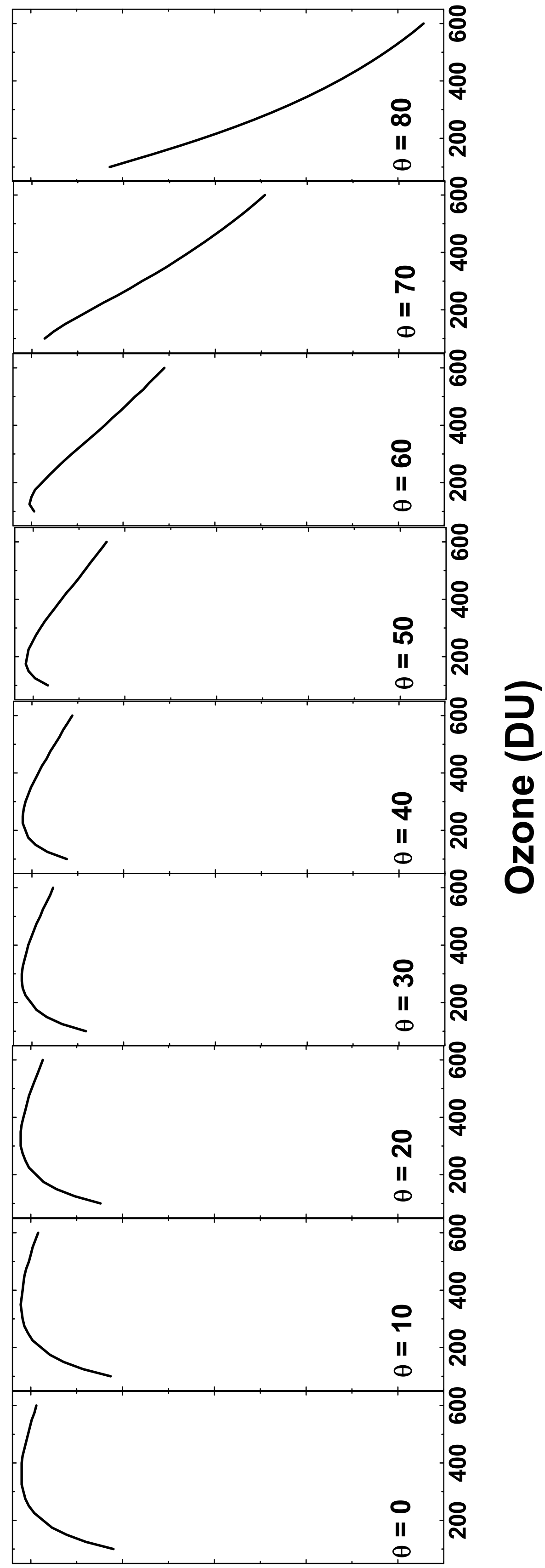

Figure A3. The RAF*(θ,Ω) function computed from RAF*$(\theta,\Omega) = \log(I_1/I_2)/\log(\Omega_2/\Omega_1)$ computed from the data shown in Figure A1.

angle (Figure A3) and is similar to the results given by *Seckmeyer et al.* [2005]. This shows the advantage of using $U(\theta)[\Omega/200]^{-RAF(\theta)}$ to define the RAF(θ) functions with no dependence on Ω.

References

Bader, K. P., and A.-B. Refat (1999), Adaptation of plants to anthropogenic and environmental stresses: The effects of air constituents and plant-protective chemicals, in *Handbook of Plant and Crop Stress*, 2nd ed., edited by M. Pessarakli, 973–1009, Marcel Dekker, New York.

Bener, P. (1972), Approximate values of intensity of natural ultraviolet radiation for different amounts of atmospheric ozone, Tech. Rep., Phys.-Meteorol. Obs. Davos, Davos Plate, Switzerland, Nat. Tech. Inf. Serv., Springfield, Va.

Bodhaine, B. A., E. G. Dutton, D. J. Hofmann, R. L. McKenzie, and P. V. Johnston (1997), UV measurements at Mauna Loa: July 1995 to July 1996, *J. Geophys. Res.*, *102*(D15), 19,265–19,273, doi:10.1029/97JD01391.

Bogh, M. K. B., A. V. Schmedes, P. A. Philipsen, E. Thieden, and H. C. Wulf (2010), Vitamin D production after UVB exposure depends on baseline Vitamin D and total cholesterol but not on skin pigmentation, *J. Invest. Dermatol.*, *130*, 546–553 doi:10.1038/jid.2009.323.

Booth, C. R., and S. Madronich (1994), Radiation amplification factors: Improved formulation accounts for large increases in ultraviolet radiation associated with Antarctic ozone depletion, in *Ultraviolet Radiation in Antarctica: Measurement and Biological Effects*, *Antarct. Res. Ser.*, vol. 62, edited by C. S. Weiler and P. S. Penhale, pp. 39–52, AGU, Washington, D. C.

Blumthaler, M., M. Salzgeber, and W. Ambach (1995), Ozone and ultraviolet-B irradiances: Experimental determination of the radiation amplification factor, *Photochem. Photobiol.*, *61*, 159–162, doi:10.1111/j.1751-1097.1995.tb03954.x.

Boucher, N., B. B. Prezelin, T. Evens, R. Jovine, B. Kroon, M. A. Moline, and O. Schofield (1994), IcecoZors '93: Biological weighting function for the ultraviolet inhibition of carbon fixation in a natural antarctic phytoplankton community, *Antarctic J.*, *29*(5).

Bouillon, R., J. Eisman, M. Garabedian, M. Holick, J. Kleinschmidt, T. Suda, I. Terenetskaya, and A. Webb (2006), *Action Spectrum for the Production of Previtamin D_3 in Human Skin, CIE 174-2006*, Int. Comm. on Illumination, Vienna, Austria.

Caldwell, M. M. (1971), Solar UV irradiation and the growth and development of higher plants, in *Photophysiology*, vol. 6, edited by A. C. Giese, chap. 4, 131–177, Academic, New York.

Camacho, I., J. Tzu, and R. S. Kirsner (2010), Regulation of Vitamin D production is independent of skin color, *J. Invest. Dermatol.*, *130*, 330, doi:10.1038/jid.2009.407.

Cullen, J. J., and P. J. Neale (1997), Biological weighting functions for describing the effects of ultraviolet radiation on aquatic systems, in *Effects of Ozone Depletion on Aquatic Ecosystems*, edited by D.-P. Haeder, pp. 97–118, R. G. Landes, Austin, Tex.

Diffey, B. L. (1991), Solar ultraviolet radiation effects on biological systems, *Rev. Physics Med. Biol.*, *36*, 299–328.

Fioletov, V. E., L. J. McArthur, T. W. Mathews, and L. Marrett (2009), On the relationship between erythemal and vitamin D action spectrum-weighted ultraviolet radiation, *J. Photochem. Photobiol.*, *95*(1), 9–16.

Flint, S. D., and M. M. Caldwell (2003), A biological spectral weighting function for ozone depletion research with higher plants, *Physiol. Plant.*, *117*, 137–144.

Ghetti, F., C. Bagnoli, and G. Checcucci (2006), Response to UV-B radiation: Weighting functions and action spectra, in *Environmental UV Radiation: Impact on Ecosystems and Human Health and Predictive Models Proceedings of the NATO Advanced Study Institute on Environmental UV Radiation*, Impact on Ecosystems and Human Health and Predictive Models, Pisa, Italy.

Grant, W. B. (2002), An estimate of premature cancer mortality in the U.S. due to inadequate doses of solar ultraviolet-B radiation, *Cancer*, *94*(6), 1867–1875.

Gruijl, F. R., H. J. C. M. Sterenborg, P. D. Forbes, R. E. Davies, C. Cole, G. Kelfkens, H. van Weelden, H. Slaper, and J. C. van der Leun (1993), Wavelength dependence of skin cancer induction by ultraviolet irradiation of albino hairless mice, *Cancer Res.*, *53*, 53–60.

Herman, J. R. (2010), Global increase in UV Irradiance during the past 30 years (1979 to 2008) estimated from satellite data, *J. Geophys. Res.*, *115*, D04203, doi:10.1029/2009JD012219.

Holick, M. F. (2004), Sunlight and vitamin D for bone health and prevention of autoimmune diseases, cancers, and cardiovascular disease, *Am. J. Clin. Nutr.*, *80*(6), 1678S–1688S.

Hollis, B. W., C. L. Wagner, M. K. Drezner, and N. C. Binkleyb (2007), Circulating vitamin D_3 and 25-hydroxyvitamin D in humans: An important tool to define adequate nutritional vitamin D status, *J. Steroid Biochem. Mol. Biol.*, *103*(3–5), 631–634.

Hülsen, G., and J. Gröbner (2007), Characterization and calibration of ultraviolet broadband radiometers measuring erythemally weighted irradiance, *Appl. Opt.*, *46*, 5877–5886.

Hunter, J. H., J. H. Taylor, and H. G. Moser (1979), Effect of ultraviolet irradiation on eggs and larvae of the northern anchovy, *Engraulis mordax*, and the pacific mackerel, *Scomber japonicus*, during the embryonic stage, *Photochem. Photobiol.*, *29*, 325–338.

Latarjet, R. (1935), Influences des variations l'ozone atmospherique sur l'activite biologique du rayonnment solaire, *Rev. Opt. Theor. Instr.*, *14*, 398–414.

Madronich, S. (1993a), The atmosphere and UV-B radiation at ground level, in *Environmental UV Photobiology*, edited by L. O. Björn, and A. R. Young, pp. 1–39, Plenum, New York.

Madronich, S. (1993b), UV radiation in the natural and perturbed atmosphere, in *Environmental Effects of UV (Ultraviolet) Radiation*, edited by M. Tevini, pp. 17–69, A. F. Lewis, Boca Raton.

Madronich, S., and S. Flocke (1997), Theoretical estimation of biologically effective UV radiation at the Earth's surface, in *Solar Ultraviolet Radiation—Modeling, Measurements and Effects*, *NATO ASI Series*, vol. I52, edited by C. Zerefos, Springer, Berlin.

Madronich, S., R. L. McKenzie, L. O. Björn, and M. M. Caldwell (1998), Changes in biologically active ultraviolet radiation reaching the Earth's surface, *Photochem. Photobiol.*, *46*, 5–19.

Mazza, C. A., H. E. Boccalandro, C. V. Giordano, D. Battista, A. L. Scopel, and C. L. Ballare (2000), Functional significance and induction by solar radiation of ultraviolet-absorbing sunscreens in field-grown soybean crops, *Plant Physiol.*, *122*, 117–125.

McKenzie, R., D. Smale, and M. Kotkamp (2004), Relationship between UVB and erythemally weighted radiation, *Photochem. Photobiol. Sci.*, *3*, 252–256.

McKinlay, A., and B. L. Diffey (1987), A reference action spectrum for ultraviolet-induced erythema in human skin; in *Human Exposure to Ultraviolet Radiation: Risks and Regulations*, *Int. Congress Ser.*, edited by W. F. Passchier, and B. F. M. Bosnajakovic, pp. 83–87, Elsevier, Amsterdam, Netherlands.

Micheletti, M. I., R. D. Piacentini, and S. Madronich (2003), Sensitivity of biologically active UV radiation to stratospheric ozone changes: Effects of action spectrum shape and wavelength range, *Photochem. Photobiol.*, *78*(5), 456–461.

Neale, P. J., and D. J. Kieber (2000), Assessing biological and chemical effects of UV in the marine environment: Spectral weighting functions, in *Causes and Environmental Implications of Increased U.V.-B. Radiation*, edited by R. E. Hester and R. M. Harrison, pp. 61–83, R. Soc. of Chem., Cambridge, UK.

Oriowo, O. M., A. P. Cullen, B. R. Chou, and J. G. Sivak (2001), Action spectrum and recovery for in Vitro UV-Induced cataract using whole lenses, *Invest. Ophthalmol. Visual Sci.*, *42*(11), 2596–2602.

Oriowo, O. M., A. P. Cullen, and J. G. Sivak (2002), Impairment of eye lens cell physiology and optics by broadband UVA/UVB radiation, *Photochem. Photobiol.*, *76*(3), 361–367.

Pessarakli, M. (1999), *Handbook of Plant and Crop Stress*, 2nd ed., Univ. of Arizona, Tucson, Ariz.

Ricchiazzi, P., S. Yang, C. Gautier, and D. Sowle (2004), SBDART: A research and teaching software tool for plane-parallel radiative transfer in the Earth's atmosphere, *Bull. Am. Meteorol. Soc.*, *79*(10), 2101–2114.

Rousseaux, M. C., C. L. Ballare, C. V. Giordano, A. L. Scopel, A. M. Zima, M. Szwarcberg-Bracchitta, P. S. Searles, M. M. Caldwell, and S. B. Diaz (1999), Ozone depletion and UVB radiation: Impact on plant DNA damage in southern South America, *Proc. Natl. Acad. Sci. U.S.A.*, *96*, 15,310–15,315.

Searles, P. S., S. D. Flint, M. M. Caldwell (2001), A meta-analysis of plant field studies simulating stratospheric ozone depletion, *Oecologia*, *127*, 1–10, doi:10.1007/s004420000592.

Seckmeyer, G., A. Bais, G. Bernhard, M. Blumthaler, C. R. Booth, K. Lantz, and R. L. McKenzie (2005), Instruments to measure solar ultraviolet radiation Part 2: Broadband instruments measuring erythemally weighted solar irradiance, *Metrologia*, *42*, 134–139.

Setlow, R. B. (1974), The wavelengths in sunlight effective in producing skin cancer: A theoretical analysis, *Proc. Natl. Acad. Sci. U.S.A.*, *71*(9), 3363–3366.

Setlow, R. B., E. Grist, K. Thompson, and A. D. Woodhead (1993), Wavelengths effective in induction of malignant melanoma, *Proc. Natl. Acad. Sci. U.S.A.*, *90*, 6666–6670.

Smith, R. C., and K. S. Baker (1982), Assessment of the influence of enhanced UV-B on marine primary productivity, in *The Role of Solar*

Ultraviolet in Marine Ecosystems, edited by J. Calkins, pp. 509–537, Plenum, New York.
Smith, R. C., et al. (1992), Ozone depletion: Ultraviolet radiation and phytoplankton biology in Antarctic waters, *Science*, *255*, 952–959.
Stolarski, R. S., and S. Frith (2006), Search for evidence of trend slowdown in the long-term TOMS/SBUV total ozone data record: The importance of instrument drift uncertainty and fingerprint detection, *Atmos. Chem. Phys. Discuss*, *6*, 3883–3912.
Taylor, H. R. (1990), Ultraviolet radiation and the eye: An epidemiological study, *Trans. Am. Ophthalmol. Soc.*, *87*, 802–853.
Tyrrell, R. M., and M. Pidoux (1987), Action spectra for human skin cells: Estimates of the relative cytotoxicity of the middle ultraviolet, near ultraviolet, and violet regions of sunlight on epidermal keratinocytes, *Cancer Res.*, *47*(7), 1825–1829.
Vermeer, M., G. J. Schmieder, T. Yoshikawa, J. W. van den Berg, M. S. Metzman, J. R. Taylor, and J. W. Streilein (1991), Effects of ultraviolet B light on cutaneous immune responses of humans with deeply pigmented skin, *J. Invest. Dermatol.*, *97*, 729–734.
Vilaplana, J. M., A. Serrano, M. Antón, M. L. Cancillo, M. Parias, J. Gröbner, G. Hülsen, G. Zablocky, A. Díaz, and B. A. de la Morena (2009), Report of the "El Arenosillo"/INTA-COST Calibration and Intercomparison Campaign of UVER Broadband Radiometers, COST Action 726, *ISBN: 978-84-692-2640-7*.
Vuilleumier, L., and J. Gröbner (2005), Operational mode uncertainty for broadband erythemal UV radiometers, *Proc. NEWRAD*, 71–72.

J. R. Herman, Goddard Space Flight Center, Greenbelt, MD 20771, USA. (jay.r.herman@nasa.gov)